Genetics and Neurobiology of Circadian Clocks in Mammals

S.M. SIEPKA,*†‡ S.-H. YOO,*†‡ J. PARK,*† C. LEE,§ AND J.S. TAKAHASHI*†¶§

*Howard Hughes Medical Institute, †Center for Functional Genomics, ¶Department of Neurobiology and Physiology, Northwestern University, Evanston, Illinois 60208; §Department of Biological Sciences, College of Medicine Florida State University, Tallahassee, Florida 32306

In animals, circadian behavior can be analyzed as an integrated system, beginning with genes and leading ultimately to behavioral outputs. In the last decade, the molecular mechanism of circadian clocks has been unraveled primarily by the use of phenotype-driven (forward) genetic analysis in a number of model systems. Circadian oscillations are generated by a set of genes forming a transcriptional autoregulatory feedback loop. In mammals, there is a "core" set of circadian genes that form the primary negative feedback loop of the clock mechanism (*Clock/Npas2, Bmal1, Per1, Per2, Cry1, Cry2,* and *CK1*ε). A further dozen candidate genes have been identified and have additional roles in the circadian gene network such as the feedback loop involving *Rev-erb*α. Despite this remarkable progress, it is clear that a significant number of genes that strongly influence and regulate circadian rhythms in mammals remain to be discovered and identified. As part of a large-scale *N*-ethyl-*N*-nitrosourea mutagenesis screen using a wide range of nervous system and behavioral phenotypes, we have identified a number of new circadian mutants in mice. Here, we describe a new short-period circadian mutant, *part-time* (*prtm*), which is caused by a loss-of-function mutation in the *Cryptochrome1* (*Cry1*) gene. We also describe a long-period circadian mutant named *Overtime* (*Ovtm*). Positional cloning and genetic complementation reveal that *Ovtm* is encoded by the F-box protein FBXL3, a component of the SKP1–CUL1–F-box protein (SCF) E3 ubiquitin ligase complex. The *Ovtm* mutation causes an isoleucine to threonine (I364T) substitution leading to a loss of function in FBXL3 that interacts specifically with the CRYPTOCHROME (CRY) proteins. In *Ovtm* mice, expression of the PERIOD proteins PER1 and PER2 is reduced; however, the CRY proteins CRY1 and CRY2 are unchanged. The loss of FBXL3 function leads to a stabilization of the CRY proteins, which in turn leads to a global transcriptional repression of the *Per* and *Cry* genes. Thus, $Fbxl3^{Ovtm}$ defines a molecular link between CRY turnover and CLOCK/BMAL1-dependent circadian transcription to modulate circadian period.

INTRODUCTION

The mechanism of circadian oscillators in mammals is generated by a cell-autonomous autoregulatory transcription-translation feedback loop (Reppert and Weaver 2002; Lowrey and Takahashi 2004; Ko and Takahashi 2006). In the primary negative feedback loop, the basic helix-loop-helix (bHLH)-PAS transcription factors, CLOCK (and its paralog NPAS2) and BMAL1 (ARNTL), dimerize and activate transcription of the *Period* (*Per1, Per2*) and *Cryptochrome* (*Cry1, Cry2*) genes (Antoch et al. 1997; King et al. 1997; Gekakis et al. 1998; Kume et al. 1999; Bunger et al. 2000; DeBruyne et al. 2007). As the PER proteins accumulate, they form complexes with the CRY proteins, translocate into the nucleus, and interact with the CLOCK/BMAL1 complex to inhibit their own transcription (Lee et al. 2001). This leads to a fall in the inhibitory complex through turnover, and the cycle starts again with a new round of CLOCK/BMAL1-activated transcription. Additional pathways in the circadian gene network such as the second negative feedback loop (involving *Rev-erb*α) in the positive limb of the oscillator are thought to add robustness to the circadian mechanism (Preitner et al. 2002; Sato et al. 2004). Finally, posttranslational modifications have critical roles in regulating the turnover, cellular localization, and activity of circadian clock proteins (Lowrey et al. 2000; Eide et al. 2005; Gallego and Virshup 2007).

Despite this progress, it is clear that a significant number of genes that strongly influence and regulate circadian rhythms in mammals remain to be discovered and identified (Shimomura et al. 2001; Takahashi 2004). Forward genetic screens have been one of the most effective tools for circadian gene discovery (Takahashi et al. 1994; Vitaterna et al. 1994; Takahashi 2004), and we have used this approach to screen the mouse genome for circadian rhythm mutants generated in the Neurogenomics Project in the Center for Functional Genomics at Northwestern University (Vitaterna et al. 2006).

MUTAGENESIS, SCREENING, AND IDENTIFICATION OF THE *PRTM* and *OVTM* GENES

In an *N*-ethyl-*N*-nitrosourea (ENU) recessive screen using the BTBR T^+ tf/J (BTBR/J) inbred mouse strain (Siepka and Takahashi 2005), we identified two mutants with short (21.4 hours) and long (25.8 hours) circadian periods in constant darkness (DD) (Fig. 1). These two mutants were named *part-time (prtm)* and *Overtime (Ovtm)* (Siepka et al. 2007), respectively. Genetic mapping of *prtm* places this mutant on chromosome 10 in the region of *Cry1* (Fig. 2A). Complementation tests of *prtm* with a *Cry1* null allele show that *prtm* is a new allele of *Cry1* (Fig. 2B). Sequencing of the *Cry1* gene in *prtm* mutants reveals a T to C mutation in the second position of the splice donor site of exon 2 causing readthrough and premature termination in intron 2 (Fig. 2C). Crosses of *prtm* with *Cry2* null mutants to produce double homozygous mutants show that these mice are arrhythmic, similar

‡These authors contributed equally to this work.

to that seen in *Cry1/Cry2* double-mutant mice (Vitaterna et al. 1999). Thus, *prtm* is a loss-of-function allele of *Cry1* and serves as a validation of the genetic screen.

The second mutant, *Ovtm*, maps to a 1.7-cM interval on chromosome 14 (Fig. 3) (Siepka et al. 2007). This region corresponds to a 4-Mb interval and contains 18 open reading frames, none of which corresponds to previously known circadian clock genes (Fig. 4A) (Lowrey and Takahashi 2004). We sequenced all annotated exons for the 18 candidate genes in the *Ovtm* interval and found only a single nonsynonymous point mutation within the coding region of *Fbxl3*. There is a single-base transition from A to G in exon 5 of *Fbxl3* in *Ovtm* mice as compared to wild-type BTBR/J mice. This mutation cosegregated perfectly with the long-period phenotype of *Ovtm*/*Ovtm* mice. The point mutation converts amino acid residue 364 from isoleucine to threonine in FBXL3 (Fig. 4A,B). This isoleucine residue is highly conserved in FBXL3 from vertebrates and in the mouse paralog FBXL21 (Fig. 4B). FBXL3 is a member of the F-box protein family with leucine-rich repeats (LRR) which is defined by its founding member, SKP2 (S-phase kinase-associated protein-2) (FBXL1) (Jin et al. 2004). SKP2 is the F-box protein moiety in the SKP1–CUL1–F-box-protein $(SCF)^{SKP2}$ E3 ubiquitin ligase complex that mediates the recognition and ubiquitination of the CDK2 inhibitor, $p27^{Kip1}$, to target it for proteasomal degradation (Cardozo and Pagano 2004). FBXL3 has 11 LRRs and can align with SKP2, which has 10 LLRs based on its protein structure; however, the carboxyl termini of SKP2 and FBXL3 are not conserved likely due to the recognition of different substrates (Hao et al. 2005). The *Ovtm* I364T mutation occurs in the carboxyl terminus of FBXL3 between LRR10 and LRR11 where the alignment with SKP2 becomes divergent (Fig. 4B). Because the LRR domains of F-box proteins are involved with substrate recognition with the SCF complex, we hypothesized that the I364T mutation could alter the interaction of FBXL3 with its substrates.

Because we isolated only one mutant allele of *Fbxl3*, and either a second independent allele, rescue, or functional evidence is required for proof in positional cloning (Takahashi et al. 1994), we used genetic complementation tests to confirm that *Ovtm* was allelic with *Fbxl3*. The crosses show that *Ovtm* and an *Fbxl3* gene trap (GT) fail to complement each other, thus providing independent and definitive evidence that *Ovtm* is an allele of *Fbxl3* (Fig. 4C). Interestingly, the period length of GT/*Ovtm* mice is indistinguishable from *Ovtm* homozygotes, suggesting that the *Ovtm* mutant allele is likely a hypomorphic or loss-of-function allele.

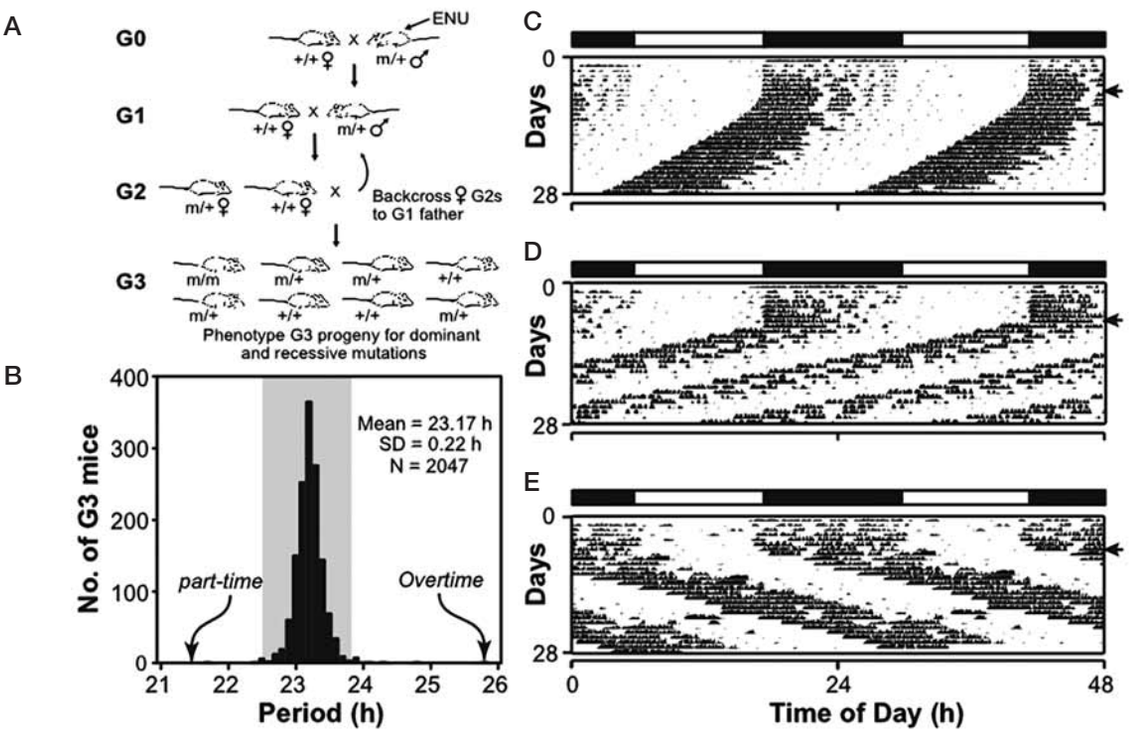

Figure 1. ENU mutagenesis screen. (*A*) Mutant mouse production. Male BTBR/J mice were treated with the chemical mutagen *N*-ethyl-*N*-nitrosourea (ENU) (1 x 250 mg/kg) and G_1 offspring were used to breed three-generation pedigrees to make ENU-induced mutations homozygous as described previously (Siepka and Takahashi 2005). (*B*) Histogram distribution of free-running period values for 3198 mice screened. (*Gray shaded area*) ±3 standard deviations (S.D.) from the mean. The original *part-time* and *Overtime* mutants are indicated by arrows. (*C*) Representative actogram of a wild-type BTBR/J mouse. The actogram is double-plotted where 48 hours of activity are represented on each horizontal line. The mice were kept on a LD12:12 cycle (*bar above*) for the first 7 days and then released into DD for 21 days (*arrowhead on the right*). (*D*) Actogram of the original *prtm* G3 mouse. The animal (a *prtm* homozygote) had a free-running period of 21.4 hours. (*E*) Actogram of the original *Ovtm* G3 mouse. The animal (an *Ovtm* homozygote) had a free-running period of 25.83 hours.

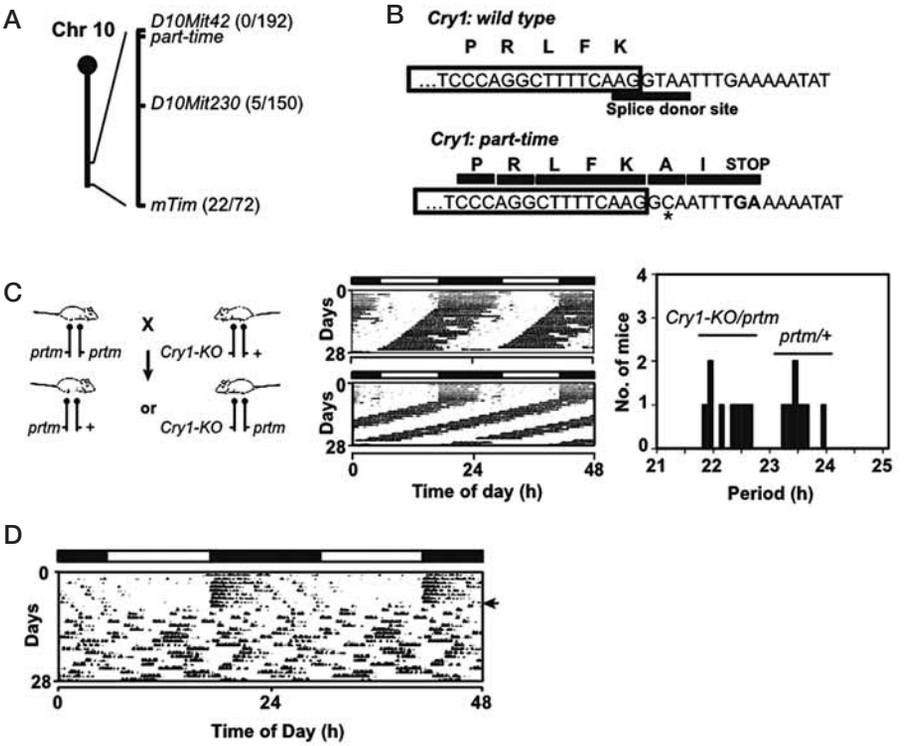

Figure 2. Genetic mapping and cloning of the *part-time* mutant. (*A*) Genetic mapping of *prtm* to chromosome 10. (*B*) The *prtm* mutation occurs within the splice donor site at the 3′ end of exon 2 of *Cry1*. (*C*) Complementation test for *prtm* and *Cry1*. (*Left panel*) Mating scheme for the complementation test. *prtm* mice were crossed to heterozygous *Cry1* knockout (*mCry1-KO*) mice. Circadian behavior was recorded for 15 progeny. The actograms are representative of *prtm*/+ (*top*) and *Cry-1KO/prtm* (*bottom*) mice. Period histogram distribution: (*left) Cry1-KO/prtm* mice (mean 22.15 hours; S.D. = 0.31; $n = 8$); (*right*) *prtm*/+ mice (mean = 23.4 hours; S.D. = 0.23; $n = 7$). Student's *t*-test (unequal variances) shows a significant difference between the two populations (DF = 13; $T = -9.12$; $p = 5.2 \times 10^{-7}$). (*D*) Representative actogram of a *prtm/prtm*, $Cry2^{-/-}$ double-mutant mouse showing an arrhythmic phenotype similar to that seen with $Cry1^{-/-}$, $Cry2^{-/-}$ double-mutant mice.

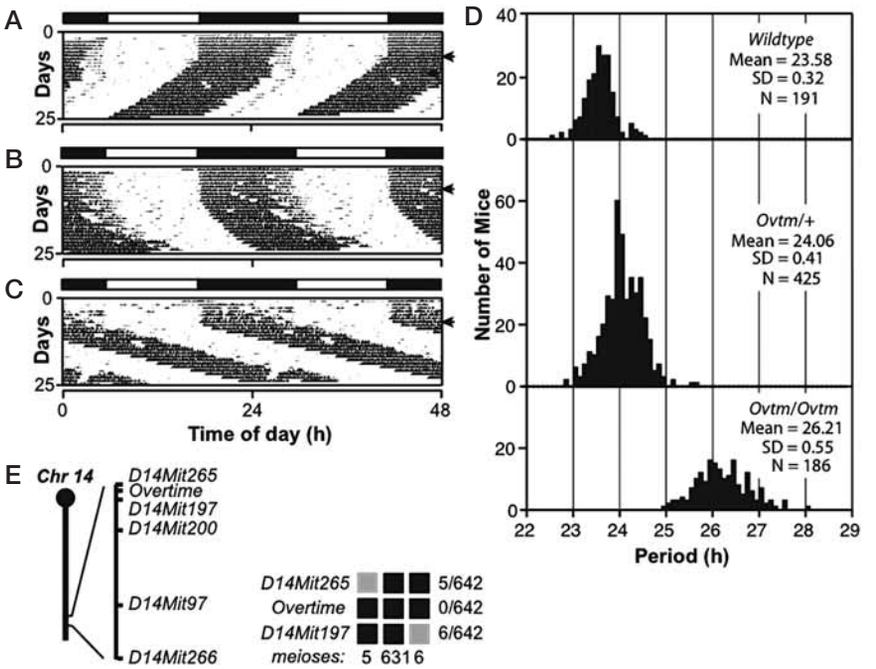

Figure 3. Semidominant phenotype of *Overtime* and genetic mapping. (*A*) Representative actograms of wild-type, (*B*) *Ovtm*/+, and (*C*) *Ovtm*/*Ovtm* [BTBR/J x C57BL/6J]F_2 mice. The actograms are plotted as described in Figure 1. (*D*) Period distribution of F_2 intercross progeny. The three panels from top to bottom represent wild-type, *Ovtm*/+, and *Ovtm*/*Ovtm* mice, respectively. (*E*) *Ovtm* maps between D14Mit265 and D14Mit197 on chromosome 14. Haplotypes of the 321 *Ovtm*/*Ovtm* F2 intercross progeny (642 meioses) are on the right. (*Black boxes*) BTBR/J alleles; (*gray boxes*) heterozygous alleles (BTBR/J and C57BL/6J). The number of recombinants per total meioses is indicated to the right of the haplotype map. (Reprinted, with permission, from Siepka et al. 2007 [©Elsevier].)

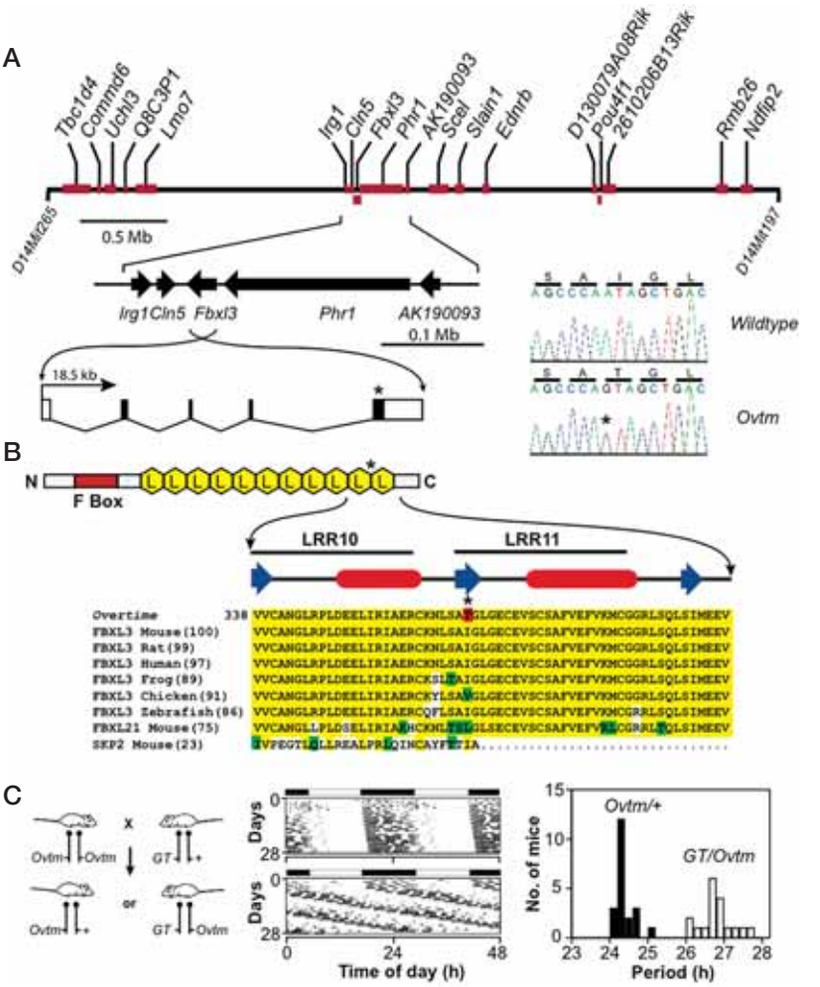

Figure 4. Positional cloning of *Overtime* and identification of *Fbxl3* mutation. (*A*) Physical map of the *Ovtm* interval. *Ovtm* maps to a 4-Mb region of chromosome 14. (*Red blocks*) Eighteen candidate genes within the interval. *Asterisks* indicate the location of the *Ovtm* mutation. (*B*) FBXL3 is an F-box protein. FBXL3 contains one F-box domain (*red box*) and 11 leucine-rich regions (LRR) (*yellow hexagons*) (Jin et al. 2004). β-strand (*blue arrow*) and α-helical (*red ovals*) regions (based on analysis using PROF in the PredictProtein server; Rost et al. 2004) of LRR10 and LRR11 are indicated above the sequence. Protein alignment: (*Yellow*) amino acid identity; (*green*) conservative substitutions; (*white*) nonconservative substitutions; (*red*) I364T *Ovtm* mutation. (*C*) Complementation test for *Ovtm* and *Fbxl3*. (*Left panel*) Mating scheme for the complementation assay. *Ovtm* mice were crossed to heterozygous *Fbxl3* gene-trap (GT) mice. Actograms are representative of *Ovtm*/+ (*top*) and GT/*Ovtm* (*bottom*) mice. Period histogram distribution: (*Black bars*) *Ovtm*/+ mice; (*white bars*) GT/*Ovtm* mice. (Reprinted, with permission, from Siepka et al. 2007 [©Elsevier].)

EFFECTS OF THE OVERTIME MUTATION ON CIRCADIAN CLOCK GENE EXPRESSION

Because FBXL3 is likely a component of an SCF E3 ubiquitin ligase complex, we examined the in vivo expression patterns of circadian clock proteins in mouse tissues to explore whether *Ovtm* might alter their abundance by affecting degradation. Figure 5A shows expression patterns of the clock proteins, CRY1, CRY2, PER1, PER2, CLOCK, and BMAL1, in liver and cerebellum. In wild-type mice, there were low-amplitude rhythms of CRY1 and CRY2 and high-amplitude rhythms of PER1 and PER2 as reported previously (Lee et al. 2001). In *Ovtm* liver tissue, CRY1 and CRY2 protein patterns were not significantly altered; however, PER1 and PER2 levels were significantly reduced (Fig. 4B). In the cerebellum, the effects of *Ovtm* were more striking. Although CRY1 levels were not different, CRY2 levels were significantly elevated in *Ovtm* mice, consistent with the hypothesis that CRY degradation is impaired. In addition, there were very clear reductions in the levels of PER1 and PER2. The reduction of PER1 and PER2 levels in *Ovtm* mice is unexpected and counterintuitive. We would have expected to see an increase rather than a decrease in protein abundance if the PER proteins were targets of FBXL3 because the *Ovtm* mutation is a loss-of-function mutation. This suggests that it is unlikely that the PER proteins are targets of FBXL3 and that the reduction in PER levels could occur as a consequence of the negative feedback on CLOCK/BMAL1-dependent transcription.

To explore the reasons for the reduction in PER1 and PER2 protein abundance, we profiled the in vivo circadian mRNA expression patterns for *Cry1, Cry2, Per1, Per2*, and *Dbp* in the liver and cerebellum of mice main-

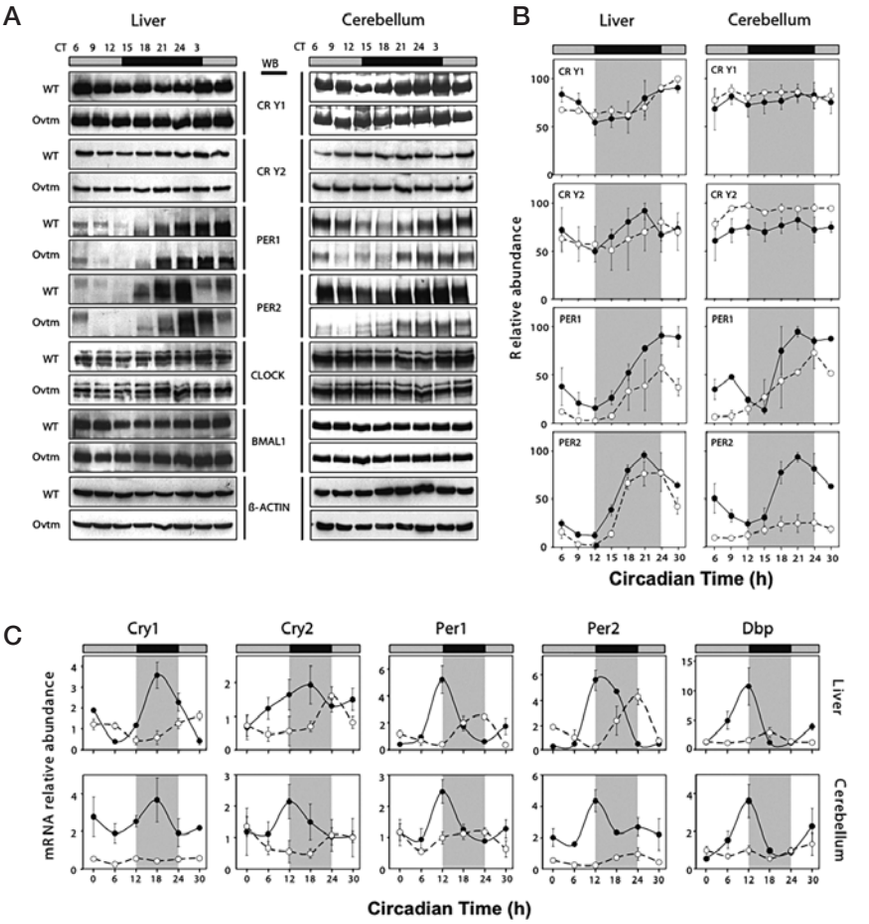

Figure 5. Altered circadian clock gene expression in *Overtime* mice. (*A*) Protein oscillation profiles of clock genes from liver and cerebellum. Wild-type and *Ovtm* mutant tissues were collected at indicated circadian times. Western blotting was performed on total protein extracts with indicated antibodies. (*B*) Quantification of proteins from liver and cerebellum. (*Closed circles*) Normalized values from wild type; (*open circles*) normalized values from *Ovtm* mice. (*C*) Real-time RT-PCR (reverse transcriptase–polymerase chain reaction) analysis for clock gene expression in wild-type and *Ovtm* mice. (*Closed circles*) Wild type; (*open circles*) values from *Ovtm* mice. All cycling genes show a significant reduction of mRNA level from *Ovtm* mice compared to wild-type mice in liver and cerebellum except for *Per2* in liver. (Reprinted, with permission, from Siepka et al. 2007 [©Elsevier].)

tained in DD. As shown in Figure 5C, the *Ovtm* mutation caused significant reductions in the mRNA abundance of all of these cycling transcripts, with the strongest effects being seen with *Cry1* and *Per2* in the cerebellum. At the mRNA level, both a delay in the peak time and a reduction in abundance can be seen. Importantly, although CRY1 and CRY2 protein levels were not lower in *Ovtm* mice, the corresponding mRNA levels for *Cry1* and *Cry2* are significantly reduced in both tissues. In addition, mRNA levels for the cycling CLOCK target gene, *Dbp* (Ripperger and Schibler 2006), were very strongly reduced in *Ovtm* mice. Thus, the mRNA profiling experiments point to an interesting and unexpected consequence of the *Ovtm* mutation: a reduction in steady-state mRNA expression of *Cry1*, *Cry2*, *Per1*, *Per2*, and *Dbp*, which are all transcriptional targets of the CLOCK/BMAL1 complex (Gekakis et al. 1998; Kume et al. 1999; Yoo et al. 2005; Ripperger and Schibler 2006).

Comparison of the effects of *Ovtm* on protein versus mRNA abundance suggests that there are two different effects on the expression of the CRY and PER proteins. The PER protein levels appear to be reduced as a consequence of reduced transcript levels. In contrast, the CRY protein levels are *not* reduced even in the face of reduced transcript levels. This suggests that potential reductions in CRY protein levels caused by reduced *Cry* transcript levels could be compensated by a reduction in protein degradation.

INTERACTION OF OVTM WITH CIRCADIAN CLOCK PROTEINS

The Pagano laboratory has found that FBXL3 targets CRY proteins for ubiquitination and degradation (Busino et al. 2007). To confirm these results and determine whether the *Ovtm* mutation affects interactions with CRY, we examined the interaction of FBXL3 or OVTM with circadian clock proteins by immunoprecipitation assays. Both FBXL3 and OVTM interacted strongly with native CRY1 and CRY2 proteins. Very weak or no interaction of FBXL3 was seen with PER1 and PER2, especially in comparison with that seen between the PERs and

β*TrCP1*, an F-box protein known to interact with the PERs (Fig. 6A) (Eide et al. 2005; Shirogane et al. 2005). In all experiments, there was a discernibly stronger interaction of the CRY proteins with FBXL3 relative to OVTM, but the difference was subtle.

We also used tagged proteins in coimmunoprecipitation assays in 293A cells which are easily transfected and express relatively low levels of clock proteins. Both FBXL3 and OVTM interacted strongly with CRY1 and CRY2 (Fig. 6B). To explore the weak interaction of FBXL3 with PER proteins, tagged *Per* constructs were also tested. All three PER proteins showed interactions with FBXL3 and OVTM, however, the strongest interactions were seen with PER2. Because PER2 interacts very strongly with CRY1 (Griffin et al. 1999; Kume et al. 1999; Lee et al. 2001), it is likely that the interactions seen here with FBXL3 may be indirect via CRY1.

EFFECTS OF OVTM ON CRY DEGRADATION

To determine whether OVTM is less efficient than FBXL3 in inducing the degradation of CRY1, we compared the effects of FBXL3 and OVTM on the stability of CRY1 following cycloheximide treatment to prevent de novo protein synthesis in transfected cells (Fig. 6C). In 293A cells, FBXL3 expression leads to the degradation of CRY1, and this degradation is blocked by the 26S proteasomal inhibitor MG132 (Fig. 6C). OVTM is less effective than FBXL3 in causing CRY1 degradation under these conditions. Interestingly, the turnover of FBXL3 is also

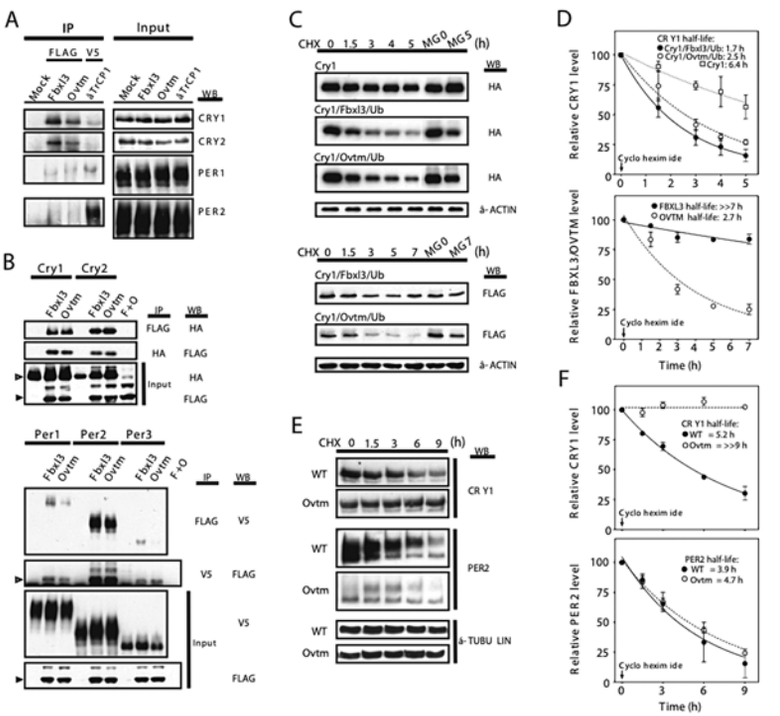

Figure 6. Interaction of FBXL3 and OVTM with circadian clock proteins. (*A*) NIH-3T3 cells were transfected with FLAG-*Fbxl3*, FLAG-*Ovtm*, and V5-β*TrCP1*. Immunoprecipitation was performed with anti-Flag or anti-V5 antibody. Native immunoprecipitated proteins were further analyzed by western blotting with anti-PER or anti-CRY antibodies. (*B*) Confirmation of interaction between FBXL3 with CRY and PER2. (*Top panel*) 293A cells were transfected with *Cry*-HA and FLAG-*Fbxl3*, FLAG-*Ovtm*. F+O is cotransfection of FLAG-*Fbxl3*, FLAG-*Ovtm*. (*Open arrowheads*) CRY; (*closed arrowheads*) FBXL3 or OVTM. (*Lower panel*) *Per*-V5 were cotransfected with FLAG-*Fbxl3*, FLAG-*Ovtm*. (*Open arrowheads*) Immunoprecipitated FBXL3 or OVTM; (*closed arrowheads*) FBXL3 or OVTM from input. (*C*) Effects of *Fbxl3* and *Ovtm* on CRY1 and FBXL3 protein stability. *Cry1*-HA was cotransfected with FLAG-*Fbxl3* or FLAG-*Ovtm* with HA-Ubiquitin (Ub). Abundance of CRY1, FBXL3, and OVTM was measured by western blotting. (*Upper panel*) Inhibition of CRY degradation by MG132 treatment plus CHX treatment; (*lower panel*) *Ovtm* mutation causes accelerated degradation of FBXL3 through the proteasomal degradation pathway. β-actin was used as a loading control. (*D*) Quantitation of the effects of *Fbxl3* and *Ovtm* on CRY1 and FBXL3 protein stability. (*Upper panel*) Effects of FBXL3 on CRY1 stability in 293A cells; (*open squares*) *Cry1* only; (*closed circles*) *Cry1* cotransfected with *Fbxl3*; (*open circles*) *Cry1* cotransfected with *Ovtm* mutant. The half-life of CRY1 is reduced by either FBXL3 (half-life: 1.7 hours) or OVTM (half-life: 2.5 hours). OVTM coexpression was less effective in CRY1 degradation compared to FBXL3. (*Lower panel*) Effect of the *Ovtm* mutation on the half-life of FBXL3; (*closed circles*) FBXL3; (*open circles*) OVTM. In the presence of CRY1, the *Ovtm* mutation caused a reduction in the protein stability of OVTM. (*E*) Stability of endogenous CRY1 and PER2 in *Ovtm* ear fibroblast cells. Protein extracts from harvested cells were analyzed with western blotting using anti-CRY1 and anti-PER2 antibody. α-tubulin was used as a loading control. (*F*) Half-life measurements of endogenous CRY1 and PER2 proteins in wild-type and *Ovtm* fibroblasts. (*Upper panel*) Time course of CRY1 levels following addition of CHX; (*closed circles*) wild-type fibroblasts; (*open circles*) *Ovtm* cells. CRY1 degradation is much more rapid in wild-type fibroblasts (half-life: 5.2 hours) than in *Ovtm* fibroblasts (>>9 hours). (*Lower panel*) Half-life measurements of PER2 proteins in wild-type and *Ovtm* fibroblasts; (*closed circles*) wild-type fibroblasts; (*open circles*) *Ovtm* fibroblasts. (Reprinted, with permission, from Siepka et al. 2007 [©Elsevier].)

affected by the OVTM mutation (Fig. 6C, bottom). FBXL3 is relatively stable with a half-life of greater than 7 hours, whereas OVTM has a much shorter half-life of 2.7 hours (Fig. 6D). Therefore, there are two effects of the OVTM mutation: a reduction in proteasome-mediated CRY1 degradation and a decreased stability of the OVTM protein itself, both of which could contribute to a loss-of-function phenotype.

To determine whether these changes in CRY1 stability seen in transfected cells are physiological, we used fibroblasts prepared from either wild-type or *Ovtm* mice and determined the half-lives of native CRY1 and PER2 proteins in these cells. As shown in Figure 6E,F, the half-life of CRY1 in *Ovtm* fibroblasts is extremely long (>>9 hours) as compared to wild-type cells (half-life = 5.2 hours). The overall levels of PER2 in *Ovtm* fibroblasts were very low, similar to that seen in the cerebellum. When the half-life of PER2 was determined, however, there was no detectable difference in the half-life of PER2 in wild-type and *Ovtm* cells (Fig. 6F). Thus, these experiments in fibroblasts from wild-type and *Ovtm* mice show that native CRY1, but not PER2, turnover is specifically altered by the *Ovtm* mutation.

CONCLUSIONS

We have shown that the ENU-induced *Overtime* mutant is caused by an I364T mutation in the mouse FBXL3 protein (Siepka et al. 2007), a member of the F-box protein with leucine-rich repeats family (Jin et al. 2004). The OVTM protein is less efficient than FBXL3 in degrading CRY1, thus providing genetic evidence that FBXL3 appears likely to be a primary F-box protein within an SCF E3 ubiquitin ligase complex (Cardozo and Pagano 2004) that targets the CRY proteins for degradation in the proteasome (Fig. 7). The I364T OVTM mutation lengthens circadian periodicity approximately 2.5 hours in mice. We propose that the phenotypic effects of the *Ovtm* mutation occur primarily through two mechanisms: (1) loss of FBXL3 function leading to stability of CRY1 protein and (2) repression of CLOCK/BMAL1-dependent transcriptional activation. These two processes lead to a striking reduction in the expression of the PER proteins which is caused by a reduction in transcription of the *Per* genes. In contrast, the levels of CRY are not reduced by the *Ovtm* mutation despite lower rates of *Cry* transcription. Because the transcription of the *Cry1* gene is strongly attenuated by the *Ovtm* mutation, it is surprising that CRY1 protein levels are not lower. The low rate of CRY1 protein degradation in *Ovtm* tissues must offset the lower synthesis of CRY1 so that the steady-state abundance of CRY1 protein is similar in *Ovtm* and wild-type mice. Importantly, however, because the turnover rate of CRY1 is reduced, the clearance of CRY1 will be prolonged even if the initial steady-state abundance levels are comparable. This would then lead to a prolongation of the CRY-dependent repression phase of the circadian cycle (Godinho et al. 2007). If such a prolongation extended CRY repression for 2–3 hours, the period-lengthening phenotype seen in *Ovtm* mice would follow as a consequence.

These results highlight the significance of an SCF^{FBXL3} E3 ubiquitin ligase complex in regulating the stability and kinetics of CRY degradation. The specificity of the FBXL3 interaction with the CRY proteins is striking and

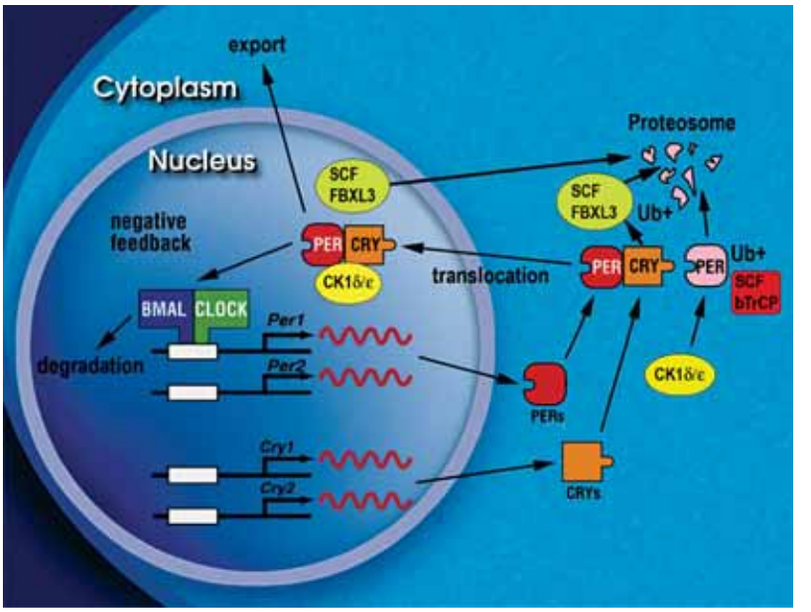

Figure 7. Model of the primary negative feedback loop within the circadian clock of mammals. Diagram shows the primary negative autoregulatory feedback loop that constitutes the circadian oscillator mechanism in mammals. The BMAL1-CLOCK heterodimeric complex activates transcription of the *Per1, Per2, Cry1*, and *Cry2* genes. The PER and CRY proteins accumulate in the cytoplasm and interact with each other and then translocate into the nucleus with CK1δ/ε where the complex interacts with BMAL1-CLOCK to inhibit the transcription of the *Per* and *Cry* genes. The turnover of the PER and CRY proteins are selectively regulated by interaction with the F-box proteins, β-TrCP and FBXL3, respectively, to target them for ubiquitination and subsequent degradation by the proteasome.

suggests that additional F-box proteins may regulate other circadian clock components. The first example of an F-box protein having a role in circadian rhythmicity was the *Arabidopsis* gene *ZEITLUPE* (*ZTL*) that encodes an F-box protein with an amino-terminal LOV domain and carboxy-terminal kelch repeats (Somers et al. 2000). *ZTL* targets the *Arabidopsis* clock protein, TOC1, for degradation by the proteasome and is thought to regulate circadian period by controlling TOC1 stability (Mas et al. 2003). In addition, the F-box protein, FKF1, mediates the cyclic degradation of CDF1, a repressor of the photoperiodic gene *CONSTANS* (Imaizumi et al. 2005), and the F-box protein, AFR, is a positive regulator of phytochrome-A-mediated light signaling in *Arabidopsis* (Harmon and Kay 2003). FBXL3 is the second example of a mammalian F-box protein regulating the circadian clock proteins. The first example is β*TrCP*, which has been shown to interact directly with the PER proteins (Eide et al. 2005; Shirogane et al. 2005). Evidence for β*TrCP* in the circadian pathway first emerged from *Drosophila* in which it was shown that *Slimb*, the ortholog of β*TrCP*, regulated circadian expression of PER and TIM (Grima et al. 2002; Ko et al. 2002). Interestingly, in *Neurospora*, the ortholog of β*TrCP*, FWD1, regulates the degradation of the clock protein, FREQUENCY (He et al. 2003). More recently, JETLAG, the *Drosophila* ortholog of Fbxl15, has been shown to have a critical role in light-induced TIM degradation by the proteasome (Koh et al. 2006). In *Drosophila*, two different SCF complexes appear to control TIM levels: a circadian pathway involving *Slimb* and a light-dependent pathway involving JET (Koh et al. 2006). It will be interesting see whether similar types of mechanisms are conserved in mammals. Because of the differences in the roles of the PER and CRY proteins in *Drosophila* and in mammals (Allada et al. 2001; Young and Kay 2001), where CRY is primarily a circadian repressor (not a photoreceptor), FBXL3 appears to function in a circadian SCF complex-mediated pathway. Unlike *Drosophila* PER, the PER1 and PER2 proteins in mammals are transcriptionally induced by light in the suprachiasmatic nucleus (SCN). It will be interesting to see whether β*TrCP* functions in a circadian or in a light-dependent SCF pathway for PER degradation (analogous to the TIM protein in *Drosophila*).

Using a forward genetics approach in mice, we have identified FBXL3 as a new molecular component of the negative feedback loop that generates circadian rhythmicity. Ironically, in the same screen, we found a second mutation in *Cry1*, the substrate for FBXL3. These experiments highlight the important role of CRY1 in the regulation of circadian period in which loss of function leads to shortened periodicity, whereas its overexpression by virtue of stabilization leads to lengthened periodicity.

ACKNOWLEDGMENTS

This chapter reports previously unpublished work describing the identification and candidate gene cloning of the *part-time* mutant and includes a shortened version of the identification and positional cloning of the *Overtime* mutant originally published by Siepka et al. (2007) in *Cell* (©Elsevier). This research was supported by National Institutes of Health grants U01 MH61915, P50 MH074924, and R01 MH078024 to J.S.T. and R01 NS053616 to C.L. J.S.T. is an investigator in the Howard Hughes Medical Institute.

REFERENCES

Allada R., Emery P., Takahashi J.S., and Rosbash M. 2001. Stopping time: The genetics of fly and mouse circadian clocks. *Annu. Rev. Neurosci.* **24:** 1091.

Antoch M.P., Song E.J., Chang A.M., Vitaterna M.H., Zhao Y., Wilsbacher L.D., Sangoram A.M., King D.P., Pinto L.H., and Takahashi J.S. 1997. Functional identification of the mouse circadian *Clock* gene by transgenic BAC rescue. *Cell* **89:** 655.

Bunger M.K., Wilsbacher L.D., Moran S.M., Clendenin C., Radcliffe L.A., Hogenesch J.B., Simon M.C., Takahashi J.S., and Bradfield C.A. 2000. Mop3 is an essential component of the master circadian pacemaker in mammals. *Cell* **103:** 1009.

Busino L., Bassermann F., Maiolica A., Lee C., Nolan P.M., Godinho S.I., Draetta G.F., and Pagano M. 2007. SCFFbxl3 controls the oscillation of the circadian clock by directing the degradation of cryptochrome proteins. *Science* **316:** 900.

Cardozo T. and Pagano M. 2004. The SCF ubiquitin ligase: Insights into a molecular machine. *Nat. Rev. Mol. Cell Biol.* **5:** 739.

DeBruyne J.P., Weaver D.R., and Reppert S.M. 2007. CLOCK and NPAS2 have overlapping roles in the suprachiasmatic circadian clock. *Nat. Neurosci.* **10:** 543.

Eide E.J., Woolf M.F., Kang H., Woolf P., Hurst W., Camacho F., Vielhaber E.L., Giovanni A., and Virshup D.M. 2005. Control of mammalian circadian rhythm by CKIepsilon-regulated proteasome-mediated PER2 degradation. *Mol. Cell. Biol.* **25:** 2795.

Gallego M. and Virshup D.M. 2007. Post-translational modifications regulate the ticking of the circadian clock. *Nat. Rev. Mol. Cell Biol.* **8:** 139.

Gekakis N., Staknis D., Nguyen H.B., Davis F.C., Wilsbacher L.D., King D.P., Takahashi J.S., and Weitz C.J. 1998. Role of the CLOCK protein in the mammalian circadian mechanism. *Science* **280:** 1564.

Godinho S.I., Maywood E.S., Shaw L., Tucci V., Barnard A.R., Busino L., Pagano M., Kendall R., Quwailid M.M., Romero M.R., O'Neill J., Chesham J.E., Brooker D., Lalanne Z., Hastings M.H., and Nolan P.M. 2007. The after-hours mutant reveals a role for Fbxl3 in determining mammalian circadian period. *Science* **316:** 897.

Griffin E.A., Jr., Staknis D., and Weitz C.J. 1999. Light-independent role of CRY1 and CRY2 in the mammalian circadian clock. *Science* **286:** 768.

Grima B., Lamouroux A., Chelot E., Papin C., Limbourg-Bouchon B., and Rouyer F. 2002. The F-box protein slimb controls the levels of clock proteins Period and Timeless. *Nature* **420:** 178.

Hao B., Zheng N., Schulman B.A., Wu G., Miller J.J., Pagano M., and Pavletich N.P. 2005. Structural basis of the Cks1-dependent recognition of p27(Kip1) by the SCF(Skp2) ubiquitin ligase. *Mol. Cell* **20:** 9.

Harmon F.G. and Kay S.A. 2003. The F box protein AFR is a positive regulator of phytochrome A-mediated light signaling. *Curr. Biol.* **13:** 2091.

He Q., Cheng P., Yang Y., Yu H., and Liu Y. 2003. FWD1-mediated degradation of FREQUENCY in *Neurospora* establishes a conserved mechanism for circadian clock regulation. *EMBO J.* **22:** 4421.

Imaizumi T., Schultz T.F., Harmon F.G., Ho L.A., and Kay S.A. 2005. FKF1 F-box protein mediates cyclic degradation of a repressor of CONSTANS in *Arabidopsis*. *Science* **309:** 293.

Jin J., Cardozo T., Lovering R.C., Elledge S.J., Pagano M., and Harper J.W. 2004. Systematic analysis and nomenclature of mammalian F-box proteins. *Genes Dev.* **18:** 2573.

King D.P., Zhao Y., Sangoram A.M., Wilsbacher L.D., Tanaka M., Antoch M.P., Steeves T.D., Vitaterna M.H., Kornhauser

J.M., Lowrey P.L., Turek F.W., and Takahashi J.S. 1997. Positional cloning of the mouse circadian *Clock* gene. *Cell* **89:** 641.

Ko C.H. and Takahashi J.S. 2006. Molecular components of the mammalian circadian clock. *Hum. Mol. Genet.* (suppl. 2) **15:** R271.

Ko H.W., Jiang J., and Edery I. 2002. Role for Slimb in the degradation of *Drosophila* Period protein phosphorylated by Doubletime. *Nature* **420:** 673.

Koh K., Zheng X., and Sehgal A. 2006. JETLAG resets the *Drosophila* circadian clock by promoting light-induced degradation of TIMELESS. *Science* **312:** 1809.

Kume K., Zylka M.J., Sriram S., Shearman L.P., Weaver D.R., Jin X., Maywood E.S., Hastings M.H., and Reppert S.M. 1999. mCRY1 and mCRY2 are essential components of the negative limb of the circadian clock feedback loop. *Cell* **98:** 193.

Lee C., Etchegaray J.P., Cagampang F.R., Loudon A.S., and Reppert S.M. 2001. Posttranslational mechanisms regulate the mammalian circadian clock. *Cell* **107:** 855.

Lowrey P.L. and Takahashi J.S. 2004. Mammalian circadian biology: Elucidating genome-wide levels of temporal organization. *Annu. Rev. Genomics Hum. Genet.* **5:** 407.

Lowrey P.L., Shimomura K., Antoch M.P., Yamazaki S., Zemenides P.D., Ralph M.R., Menaker M., and Takahashi J.S. 2000. Positional syntenic cloning and functional characterization of the mammalian circadian mutation tau. *Science* **288:** 483.

Mas P., Kim W.Y., Somers D.E., and Kay S.A. 2003. Targeted degradation of TOC1 by ZTL modulates circadian function in *Arabidopsis thaliana*. *Nature* **426:** 567.

Preitner N., Damiola F., Lopez-Molina L., Zakany J., Duboule D., Albrecht U., and Schibler U. 2002. The orphan nuclear receptor REV-ERBalpha controls circadian transcription within the positive limb of the mammalian circadian oscillator. *Cell* **110:** 251.

Reppert S.M. and Weaver D.R. 2002. Coordination of circadian timing in mammals. *Nature* **418:** 935.

Ripperger J.A. and Schibler U. 2006. Rhythmic CLOCK-BMAL1 binding to multiple E-box motifs drives circadian Dbp transcription and chromatin transitions. *Nat. Genet.* **38:** 369.

Rost B., Yachdav G., and Liu J. 2004. The PredictProtein server. *Nucleic Acids Res.* **32:** W321.

Sato T.K., Panda S., Miraglia L.J., Reyes T.M., Rudic R.D., McNamara P., Naik K.A., FitzGerald G.A., Kay S.A., and Hogenesch J.B. 2004. A functional genomics strategy reveals Rora as a component of the mammalian circadian clock. *Neuron* **43:** 527.

Shimomura K., Low-Zeddies S.S., King D.P., Steeves T.D., Whiteley A., Kushla J., Zemenides P.D., Lin A., Vitaterna M.H., Churchill G.A., and Takahashi J.S. 2001. Genome-wide epistatic interaction analysis reveals complex genetic determinants of circadian behavior in mice. *Genome Res.* **11:** 959.

Shirogane T., Jin J., Ang X.L. and Harper J.W. 2005. SCFbeta-TRCP controls clock-dependent transcription via casein kinase 1-dependent degradation of the mammalian period-1 (Per1) protein. *J. Biol. Chem.* **280:** 26863.

Siepka S.M. and Takahashi J.S. 2005. Forward genetic screens to identify circadian rhythm mutants in mice. *Methods Enzymol.* **393:** 219.

Siepka S.M., Yoo S.H., Park J., Song W., Kumar V., Hu Y., Lee C., and Takahashi J.S. 2007. Circadian mutant *Overtime* reveals F-box protein FBXL3 regulation of cryptochrome and period gene expression. *Cell* **129:** 1011.

Somers D.E., Schultz T.F., Milnamow M., and Kay S.A. 2000. ZEITLUPE encodes a novel clock-associated PAS protein from *Arabidopsis*. *Cell* **101:** 319.

Takahashi J.S. 2004. Finding new clock components: Past and future. *J. Biol. Rhythms* **19:** 339.

Takahashi J.S., Pinto L.H., and Vitaterna M.H. 1994. Forward and reverse genetic approaches to behavior in the mouse. *Science* **264:** 1724.

Vitaterna M.H., Pinto L.H., and Takahashi J.S. 2006. Large-scale mutagenesis and phenotypic screens for the nervous system and behavior in mice. *Trends Neurosci.* **29:** 233.

Vitaterna M.H., King D.P., Chang A.M., Kornhauser J.M., Lowrey P.L., McDonald J.D., Dove W.F., Pinto L.H., Turek F.W., and Takahashi J.S. 1994. Mutagenesis and mapping of a mouse gene, Clock, essential for circadian behavior. *Science* **264:** 719.

Vitaterna M.H., Selby C.P., Todo T., Niwa H., Thompson C., Fruechte E.M., Hitomi K., Thresher R.J., Ishikawa T., Miyazaki J., Takahashi J.S., and Sancar A. 1999. Differential regulation of mammalian period genes and circadian rhythmicity by cryptochromes 1 and 2. *Proc. Natl. Acad. Sci.* **96:** 12114.

Yoo S.H., Ko C.H., Lowrey P.L., Buhr E.D., Song E.J., Chang S., Yoo O.J., Yamazaki S., Lee C., and Takahashi J.S. 2005. A noncanonical E-box enhancer drives mouse Period2 circadian oscillations in vivo. *Proc. Natl. Acad. Sci.* **102:** 2608.

Young M.W. and Kay S.A. 2001. Time zones: A comparative genetics of circadian clocks. *Nat. Rev. Genet.* **2:** 702.